



King Saud University

Arabian Journal of Chemistry

www.ksu.edu.sa  
www.sciencedirect.com



ORIGINAL ARTICLE

# Fabrication of $\beta$ -cyclodextrin and sialic acid copolymer by single pot reaction to site specific drug delivery



Parbeen Singh <sup>a,b</sup>, Xiaohong Ren <sup>a</sup>, Yaping He <sup>a,b</sup>, Li Wu <sup>a</sup>, Caifen Wang <sup>a</sup>, Haiyan Li <sup>a</sup>, Vikramjeet Singh <sup>a,c,\*</sup>, Jiwen Zhang <sup>a,b,\*</sup>

<sup>a</sup> Center for Drug Delivery System, Shanghai Institute of Materia Medica, Chinese Academy of Sciences, Shanghai 201203, China

<sup>b</sup> University of Chinese Academy of Sciences, Beijing 100049, China

<sup>c</sup> School of Pharmaceutical Sciences, Sun Yat-Sen University, Guangzhou 510006, China

Received 12 September 2017; accepted 19 November 2017

Available online 24 November 2017

## KEYWORDS

Sialic acid;  
Cyclodextrin;  
Supramolecular copolymer;  
Site specific drug delivery

**Abstract** The fabrication of supramolecular host in combination biomolecules is an interesting idea in modern drug delivery for development of new polymer with advanced chemical and biological properties. Herein, hyper-crosslinked copolymer was fabricated from  $\beta$ -cyclodextrin ( $\beta$ -CD) and sialic acid (SA) monomers, which can be undoubtly considered as a new class of copolymer. The as-synthesized copolymer has complexation properties, which could cover the drug within the structure and deliver to the site of action. The well-known inclusion capability of  $\beta$ -CD and targeted efficacy of SA made it more appropriate for targeted drug delivery. The copolymer was characterized using a wide range of spectroscopic and microscopic techniques such as synchrotron radiation based FTIR spectroscopy (SR-FTIR), differential scanning calorimetry (DSC), thermogravimetric analysis (TGA), and powder X-ray diffraction (PXRD). The surface area and porosity were calculated by using Nitrogen adsorption method. Doxorubicin (Dox) was selected as a model drug to evaluate the loading efficiency and cellular penetration ability of the copolymer. The copolymer showed high adsorption towards Dox with no significant cytotoxic effects on HeLa cells as proved by cell viability assay. High cellular penetration of Dox loaded copolymer was also recorded by confocal microscopy when compared with free Dox in HeLa cells at 4 h of exposure.

\* Corresponding authors at: Center for Drug Delivery Systems, Shanghai Institute of Materia Medica, Chinese Academy of Sciences, No. 501 of Haili Road, Shanghai 201203, China.

E-mail addresses: [singh.simm@outlook.com](mailto:singh.simm@outlook.com) (V. Singh), [jwzhang@simm.ac.cn](mailto:jwzhang@simm.ac.cn) (J. Zhang).

Peer review under responsibility of King Saud University.



Production and hosting by Elsevier

Thus,  $\beta$ -CD-SA copolymer could be a useful carrier for targeted drug delivery of cancer and has the potential for further investigation in viral and nervous disease due to the targeting ability of SA. © 2017 Production and hosting by Elsevier B.V. on behalf of King Saud University. This is an open access article under the CC BY-NC-ND license (<http://creativecommons.org/licenses/by-nc-nd/4.0/>).

## 1. Introduction

The conventional drug delivery systems to target the specific site are limited by non-targeted properties of the drug carriers, metabolism of active drugs during circulation, stability and solubility of drugs, and cytotoxic nature of drug carriers (Hare et al., 2017; Shi et al., 2017). Polymers are historically dominated material in medicine and successfully applied as carriers for kind of drug delivery purposes. Supramolecular assembly of bioactive and non-bioactive molecules or co-assembly of drug with its vehicle has great potential in the search for functional systems. These supramolecular biomolecules have been used for tissue engineering, cell mimetic, and target the specific site with biofriendly nature (Freeman et al., 2015; Rudra et al., 2010; Webber et al., 2016). Cyclodextrins (CDs) are a family of cyclic oligosaccharides with a hydrophilic outer surface and a lipophilic central cavity that have been used as multifunctional drug carriers (Crini, 2014; Hirayama and Uekama, 1999; Hirotsu et al., 2017; Uekama, 1999). In addition to the parental CDs ( $\alpha$ -CD,  $\beta$ -CD, and  $\gamma$ -CD), the commonly available derivatives including HP- $\beta$ -CD, SBE- $\beta$ -CD, and methyl  $\beta$ -CD have been also used in pharmaceuticals due to their special physicochemical properties (Alupei et al., 2005; Mendez-Ardoy et al., 2011). Especially,  $\beta$ -CD has been used to fabricate nanogels (Kettel et al., 2012), nanoparticles (Gil et al., 2012), high performance oral drug delivery carriers (Zhang et al., 2015), taste masking agents, nanofibers (Chen et al., 2011), siRNA delivery carriers (O'Mahony et al., 2012), gene delivery carriers (Wang et al., 2010), and nanospikes as drug delivery carrier [13]. CDs crosslinked polymers are a class of hyper-reticulated polymeric materials used in pharmaceutical and gas storage applications (Cavalli et al., 2010; Russo et al., 2016). These crosslinked polymers reported for enhancement of solubility and bioavailability (Ansari et al., 2011; Darandale and Vavia, 2013; Minelli et al., 2012; Rao et al., 2013; Torne et al., 2013). The noncovalent interaction through host-guest mechanism with guest molecules makes CDs potent carriers for various purposes.

Copolymerization of CDs is an interesting area to fabricate sophisticated drug carriers with advanced properties. Meo and coworkers reported cyclodextrin-calixarene copolymer which shows good absorption abilities towards nitroarenes (Lo Meo et al., 2014). Poly (methyl vinyl ether-co-maleic anhydride)-graft-hydroxypropyl- $\beta$ -cyclodextrin amphiphilic copolymer showed 20 folds enhancement in bioavailability of FK506 (Zhang et al., 2015). The copolymer of CD and chitosan used for DNA and siRNA delivery showed good ability to condense pDNA into nanoparticle with much lower cytotoxicity and superior transfection activity in comparison with monomers (Ping et al., 2011). In another research,  $\beta$ -CD-amphiphilic copolymer grafted with poly lactic acid (PLA) and polyethylene glycol (PEG) was used in hydrophobic anti-cancer drug delivery which shows pH responsive sustainable

release with high fluorescence intensity of drug inside the cells (Xu et al., 2015).

The functionalization of CDs by crosslinking with bioactive moiety improves their therapeutic properties. Herein, we selected 5-acetyl neuraminic acid or specially called sialic acid (SA) in this report for this purpose. SA is well known for effective block improvement in the antigenic site or recognition marker on the cell surface and protection them from degradation by surrounding immune system. SA is anionic monosaccharide 9-carbon sugar commonly located at the cell surface and can be used as a ligand to target and detection of various type cancer cells (Lee et al., 2006; Perillo et al., 1998). The role of SA in the cells is, participant in carbohydrate-protein interaction to mediate recognition phenomenon. SA has properties to bind with sialic acid binding immunoglobulin like lectin (Siglec) family which are immunomodulatory receptor expressed by immune cells (Bull et al., 2017). SA was previously used for biochemical engineering purpose of cell surface (Buttner et al., 2002). It was successfully used to decorate the PLGA nanoparticles for targeted drug delivery (Bondioli et al., 2010). Owing to SA's monosaccharide structure and freely available hydroxyl and carboxyl groups, other than a conventional surface modification with SA, we envisaged to fabricate the  $\beta$ -CD-SA copolymer using diphenyl carbonate (DPC) as a cross-linking agent. The targeting efficacy of SA in the copolymer and drug loading properties from monomer  $\beta$ -CD are especially of interest to be confirmed for various directional drug delivery purpose.

The aim of this research was to fabricate the copolymer of SA with  $\beta$ -CD and evaluate the feasibility for targeted drug delivery purpose. The  $\beta$ -CD-SA copolymer was successfully synthesized using one step carbonate linking reaction and fully characterized using various techniques including, SR-FTIR, DSC, TGA, and PXRD. For the proof of concept, the most studied anticancer drug, Dox (Minotti et al., 2004; Sultana et al., 2010), was selected as a model compound to test the loading and cellular uptake efficiency. The HeLa cells were used to evaluate the cell viability assay and *in vitro* cellular uptake study of free Dox and Dox loaded  $\beta$ -CD-SA copolymer.

## 2. Experimental

### 2.1. Materials

The  $\beta$ -cyclodextrin was purchased from Anhui Sunhere Pharmaceutical Excipients Co. Ltd., diphenyl carbonate was purchased from Shanghai Aladdin Bio-Chem Technology Co. Ltd., and cell eagle medium and fetal bovine serum (FBS) were purchased from Thermo Fisher Scientific USA. Sialic acid was obtained from Huzhou Xinaote Pharmaceutical & Chemical Ltd. All organic solvents and chemicals including dimethyl formamide (DMF), triethylamine (TEA) were of analytical grade purchased from Sinopharm Chemical Reagents Co. Ltd. and

used without further purification. HeLa cervical carcinoma cells line were obtained from the cell bank of Chinese Academy of Sciences SIMM, China. Cell labeling dye DAPI H-1200 was purchased from Vector Laboratories Inc. USA. MTT reagents were purchased from Gibco Thermo Fisher Scientific Ltd.

## 2.2. Synthesis of $\beta$ -CD-SA copolymer

A facile procedure was adopted for the  $\beta$ -CD-SA copolymer synthesis according to the previously reported method of cyclodextrin crosslinking by DPC (Trotta et al., 2012). For synthesis process, 30 mM solution (10 mL) of each  $\beta$ -CD (340 mg) and SA (92 mg) in DMF (10 mL) was prepared in a clean and dry round bottom flask and heated up to 80 °C to obtain a clear solution. DPC was added subsequently to the flask and stirred for 10 mins. Finally, 300  $\mu$ L of triethylamine (TEA) was also added followed by stirring at 400 RPM for 12 h. The TEA was used as a catalyst to facilitate the reaction. After completion of polymerization reaction, the crude mass was cooled to the room temperature and washed with 60 mL distilled water to get the precipitation of crude copolymer. The reaction crude was then thoroughly washed in ethanol (Soxhlet) and distilled water to remove unreacted reagents and by-products especially phenol. The product was subsequently lyophilized for 12 h using freeze dryer (SIM international group Co., Ltd., USA). The amount of catalyst (TEA) and reaction time (12 h) were set as minimum values required for the copolymer production after complete validation.

## 2.3. Characterization methods

FTIR spectroscopy of all samples was recorded by using synchrotron radiation based Thermo-scientific system Nicolet™ iS™5 FT-IR Spectrophotometer (SR-FTIR) in the region of 4000–650  $\text{cm}^{-1}$ . The IR spectra of SA and  $\beta$ -CD were also recorded as controls to compare with that of the copolymer for structure confirmation. All samples were processed by OMNIC software.

The synthesized product was characterized by microscopic and spectroscopic methods. Particle size and zeta potential of copolymer particle were measured by Malvern Zetasizer, Nano series (Nano ZS90). All samples were measured in triplicates.

The thermal profile of copolymer was recorded using differential scanning calorimeter (DSC 822, Mettler Toledo, Switzerland). About 2.0 mg of each sample was heated in a pierced aluminum pan from 50 °C to 300 °C with a heating rate of 10 °C  $\text{min}^{-1}$ . Thermal data analyses of the DSC thermal profiles were conducted using Mettler Toledo STAR system software. TGA was carried out in Perkin-Elmer Pyris-1 TGA equipment, using dry air with a nitrogen gas flow of 20 mL  $\text{min}^{-1}$  and a scan rate of 10 °C  $\text{min}^{-1}$ . Samples were weighed (approximately 5 mg) in a hanging aluminum pan and the weight loss percentage of the samples was monitored from 40 to 600 °C. The obtained data were processed by star pyris software. The data were further processed with Origin Pro 8 software.

The lyophilized samples were used for the powder X-ray diffraction (PXRD) analysis measurement to keep the originality of internal structure. The particles were examined by PXRD using a D8 Advance (Bruker, Germany) with a locked

coupled scan type. The scan speed was 0.1 s per step and the increment was 0.021. The running conditions were 40 kV, 40 mA, and the scan range was from 3 to 40°.

Nitrogen adsorption-desorption isotherm was measured with a liquid nitrogen bath (−196 °C) using a porosimeter (TriStar 3000 V6.05 A, USA). In order to remove the interstitial solvents, the samples were activated by immersing in DCM for three days and dried under vacuum at 50 °C for 12 h. Known amounts of samples (e. g. 150–200 mg) were loaded into the sample tubes and degassed under vacuum (10<sup>−5</sup> Torr) at 100 °C for 5 h. Brunauer–Emmett–Teller (BET) model was applied to measure the specific surface areas of the samples. The pore size of the copolymer was analyzed by Barrett, Joyner, Halenda (BJH) model.

## 2.4. Monomer composition ratio

The determination of chemical composition is the most fundamental type of characterization in copolymer although there is molecular weight distribution is important as well as chemical composition. The HPLC is a most sophisticated technique used for determination of composition ratio distribution of copolymer. The composition ratio of SA in the copolymer was determined by HPLC (Agilent Technology, 1290 infinity) with evaporative light scattering detector (ELSD) (model- Agilent Technology, 1260 ELSD). The SA was recovered from copolymer by hydrolysis of ester and anhydride bond using ammonia (NH<sub>3</sub>). Briefly, 30 mg of copolymer samples dispersed into 1 mL aqueous solution of ammonia (80:20). After 20 min sonication, 2 mL of water was added to dilute the solution and sonicated for 5 mins. The samples were centrifuged at 12,000 RPM and filtered through 0.22  $\mu$ m filter membrane and injected into HPLC. Standard samples of SA prepared in the same way by using 3.0 mg of standard SA. The details of HPLC method are listed in ESI.

## 2.5. Drug adsorption

The Dox was taken into account for optimization of drug adsorption efficiency and cellular uptake study. Distilled water was used as a medium for loading experiments due to Dox good aqueous solubility. In loading experiments, 100 mg of the copolymer was incubated with 25 mL of 0.5 mg  $\text{mL}^{-1}$  aqueous Dox solution. During shaking (100 RPM) at room temperature, samples were taken at different time period till for 8 h and centrifuged (10,000 RPM), the supernatant was evaluated for loading capacity. The HPLC method was used for Dox is listed in ESI. The concentration of drug and shaking time was also set up after validation and drug loading capacity of  $\beta$ -CD-SA copolymer was calculated according to formula (1)

$$\text{Drug loading (\%)} = \frac{D_t - D_r}{D_t} \times 100 \quad (1)$$

where D<sub>t</sub> is the total amount of drug in solution, D<sub>r</sub> is the drug amount in the supernatant layer.

## 2.6. Cell viability study

The HeLa cells obtained from cell bank of Chinese Academy of Sciences and further sub-cultured as per protocol listed in

ESI. To determine the *in vitro* cytotoxicity of the  $\beta$ -CD-SA copolymer, HeLa cells were seeded into 96-well plates and incubated for 24 h with samples (10  $\mu$ L). MTT stock solution (5 mg  $\text{mL}^{-1}$ ) was then added to each well and incubated for 4 h. At the end of the experiment, the medium was replaced with DMSO to dissolve the formazan crystal and the absorbance was measured at 490 nm using microplate reader (Thermo scientific, Multiscan Go). The cell viability was calculated by using following formula (2):

$$\text{Cell Viability (\%)} = \frac{\text{OD}_{\text{exp}} - \text{OD}_{\text{blank}}}{\text{OD}_{\text{control}} - \text{OD}_{\text{blank}}} \times 100 \quad (2)$$

### 2.6.1. Cellular uptake study

To determine the cellular uptake, the cells were incubated with Dox and Dox loaded  $\beta$ -CD-SA copolymer particles at 37 °C for 4 h. To determine the intracellular localization of  $\beta$ -CD-SA copolymer particles in HeLa cells, the cells were seeded into 8 well-chambered glasses and incubated with free Dox and Dox loaded  $\beta$ -CD-SA copolymer particles for 4 h, and the cells were labeled with DAPI H-1200 to identify the lysosomes and nucleus. Intracellular localization was recorded by confocal microscopy (Leica microscopic system) and confocal images were processed by LAS-X software.

## 3. Results and discussion

### 3.1. Synthesis of $\beta$ -CD-SA copolymer

In order to accomplish the  $\beta$ -CD-SA copolymer synthesis, different approaches from previously reported literature have exploited. The easily accessible crosslinking between sialic acid and  $\beta$ -CD have done by crosslinking between secondary hydroxy groups of  $\beta$ -CD and carboxyl and a secondary hydroxyl group of SA groups through DPC via carbonyl bond. The DPC has been reported as a suitable electrophile for crosslinking and able to produce carbonyl bond between the hydroxyl groups of two monomers (Binello et al., 2008; Oba et al., 2000). Due to the occurrence of polysubstitution side process, the reaction produced a mixture of products which bear the different number of by-products.

In order to synthesise the copolymer, the predetermined molar ratio of  $\beta$ -CD: DPC: SA were reacted in DMF to get the final  $\beta$ -CD-SA copolymer. All the by-products and catalyst of the reaction were thoroughly washed with water and ethanol. The final product was purified by a soxhlet extraction

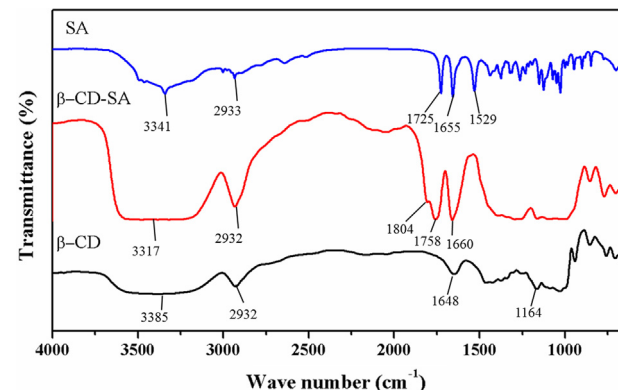


**Fig. 2** SR-FTIR spectra of  $\beta$ -CD-SA copolymer show the presence of carbonyl bond between two monomers. The peaks at 1804  $\text{cm}^{-1}$  and 1750  $\text{cm}^{-1}$  show the successful formation of carbonyl bond between two monomers.

(6h) method using ethanol to remove the traces of phenol from the copolymer.

### 3.2. Copolymer characterization

#### 3.2.1. FTIR characterization

Preliminary spectroscopic characterization of  $\beta$ -CD-SA immediately confirmed the presence of ester and anhydride carbonyl bond between  $\beta$ -CD and SA. The possible structure of copolymer was diagrammatically designed with help of Chem Draw software (Fig. 1). The SR-FTIR spectra of monomers and  $\beta$ -CD-SA copolymer depicted in Fig. 2. The IR spectra of SA showed absorption stretching band of an amide group (N—H) and a hydroxyl group at between 3340 and 3500  $\text{cm}^{-1}$ , —CH<sub>2</sub> group observed at near 2933  $\text{cm}^{-1}$  and carbonyl (C=O) group of amide group observed at 1650  $\text{cm}^{-1}$ . The carbonyl bond peak of the carboxylic acid observed at 1725  $\text{cm}^{-1}$ . The  $\beta$ -CD-SA copolymer showed a characteristic broad stretching of carbonyl bond of anhydride between a carboxylic acid group of SA and hydroxyl group of  $\beta$ -CD, at 1804  $\text{cm}^{-1}$ . The second bond of the copolymer was predicted as an ester bond between the hydroxyl group of both monomers was observed at 1758  $\text{cm}^{-1}$ . The FTIR spectra showed the successful linkage of  $\beta$ -CD and SA as we predicted.

The average particle size and average zeta potential of copolymer particles were recorded as 441  $\pm$  30 nm and -21

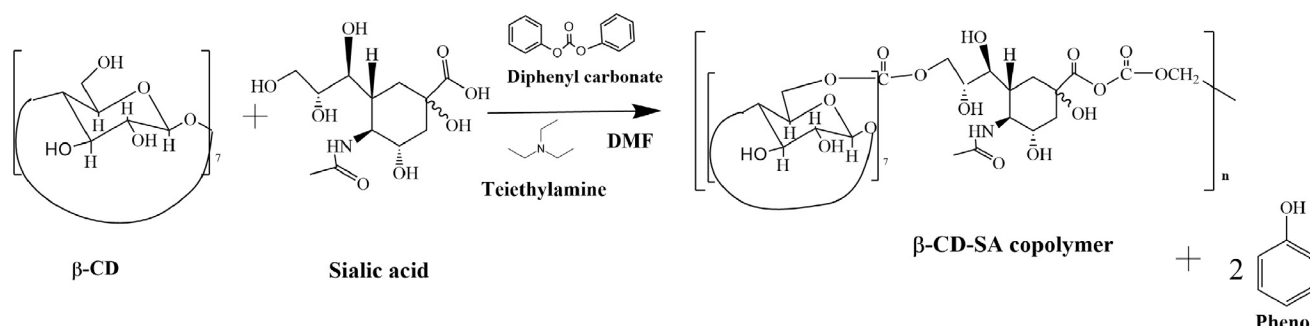


**Fig. 1** Diagrammatic representation of reaction and structure of  $\beta$ -CD-SA copolymer.

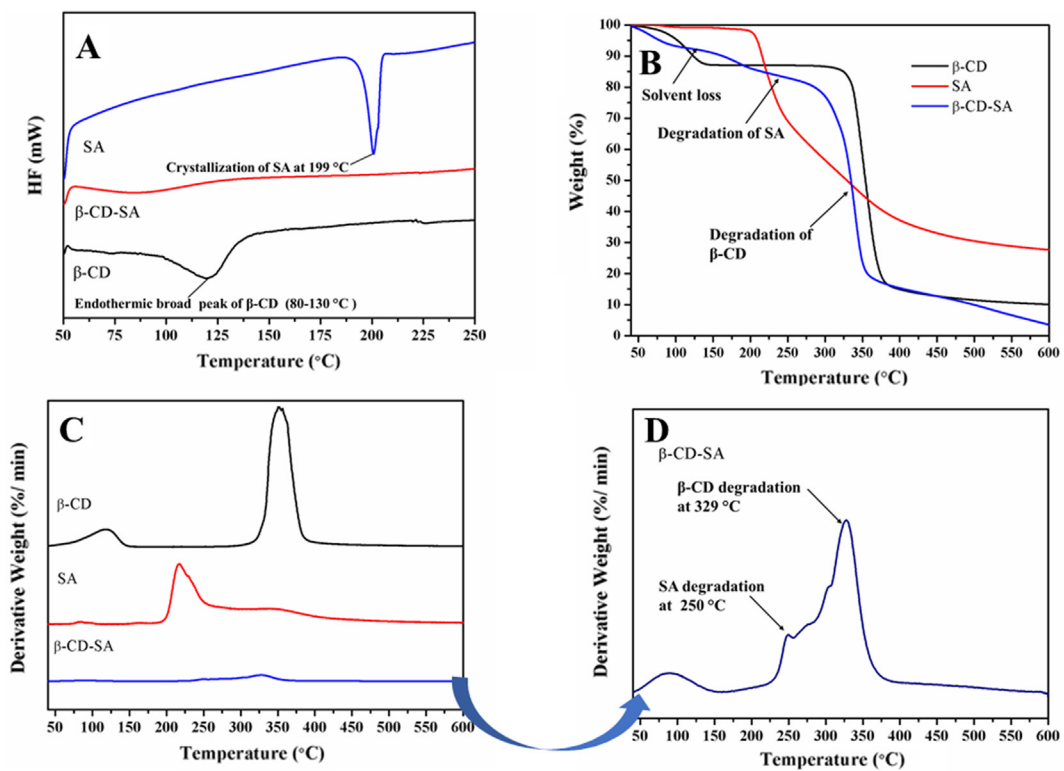


**Fig. 3** DSC (A) and TGA (B) graphs of  $\beta$ -CD-SA copolymer indicate the better thermal stability of copolymer than its monomer (SA and  $\beta$ -CD). The DTG graph of all samples (C) and copolymer (D) show the copolymer contains both monomers degradation peaks.

$\pm 2$  mV, respectively, which confirmed good stability of the copolymer.

### 3.3. Thermal behavior study

The obtained  $\beta$ -CD-SA copolymer was thermally evaluated by DSC and TGA techniques and obtained graphs are shown in Fig. 3. The  $\beta$ -CD-SA copolymer exhibits different thermal properties when compared with the monomers ( $\beta$ -CD and SA). The results of DSC were interpreted in accordance with a previous report (Eastman, 1998). The shape of the DSC curve was recorded very different from that DSC peaks of parent compounds. The parent compound,  $\beta$ -CD, showed a broad endothermic peak for dehydration between 80 and 130 °C whereas, SA crystallization peak was observed at 198 °C. Overall, it could be seen that the  $\beta$ -CD-SA copolymer displayed phase transition that corresponds to amorphous solid material and did not show any specific peak. It must be mentioned that in all cases the samples showed extensive degradation on heating (curves were not reversible on cooling and carbonized residue was always found at the end of the experiment). The DSC data also showed the amorphous nature of this copolymer as later confirmed by PXRD.

Thermal stability is an important requirement in view of any possible application of copolymer. TGA under the nitrogen atmosphere was used to determine the thermal degradation of the  $\beta$ -CD-SA copolymer and the two monomers. The TGA curve of copolymer showed an initial loss of solvent and one sharp degradation step, centered at 350 °C, accounted nearly 92 % mass loss. Thus the crosslinked copolymer was

recorded more thermally stable. Subsequently heating up to 600 °C resulted in almost 96 % degradation of the copolymer. While the parent compounds SA showed quite different thermal properties than the copolymer showed the copolymer contains less part of SA. The most part of copolymer contained by  $\beta$ -CD and followed similar degradation pattern.

The DTG data of copolymer (Fig. 3C & D) show the two step weight loss of the copolymer. The copolymer showed the initial degradation of SA due to low melting point at 250 °C and 270 °C followed by degradation peak of  $\beta$ -CD centered at 329 °C. Herein, the thermal study shows that the ther-

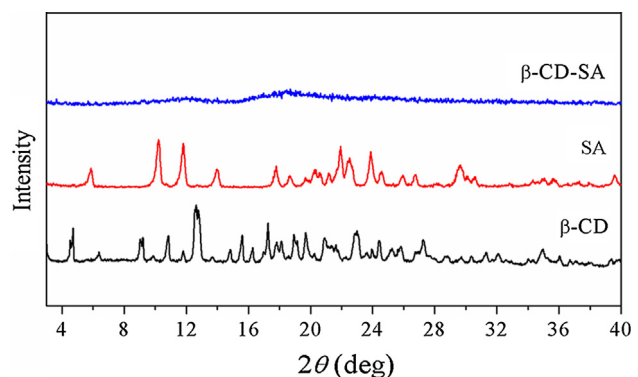


**Fig. 4** PXRD graph represents the amorphous nature of  $\beta$ -CD-SA copolymer. The crystallinity of parent compounds lost after crosslinking.

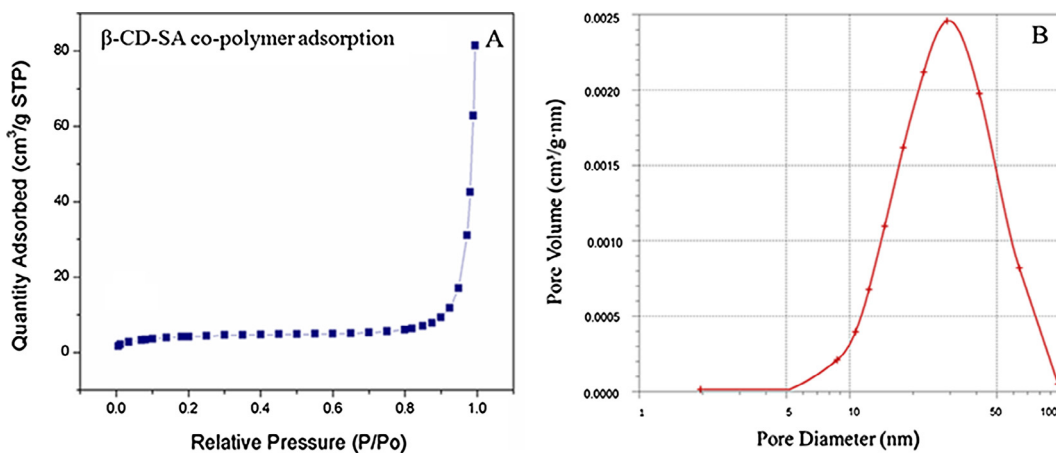


**Fig. 5** BET adsorption curve and pore size distribution of  $\beta$ -CD-SA copolymer. The graph (A) shows the  $N_2$  adsorption and (B) represents the large pore diameter of the copolymer.

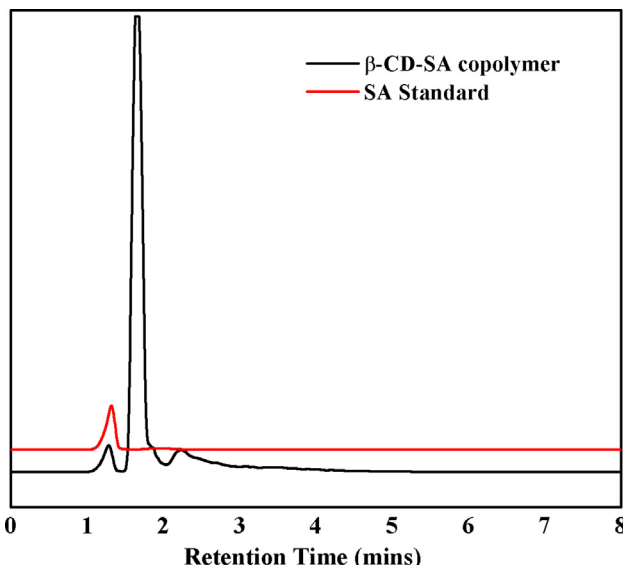


**Fig. 6** HPLC chromatogram showing the peak of SA in copolymer along with  $\beta$ -CD after hydrolysis of chemical bonds. The chromatogram was obtained employing ELSD detector.

mal stability of copolymer, as well as extensive degree of crosslinking, has been achieved in ideal composition.

#### 3.4. Crystallinity study by PXRD

Since PXRD is a useful technique to understand the crystalline behavior of compounds, it is most widely used for crystal structure determination. The PXRD spectra of  $\beta$ -CD-SA copolymer showed no specific diffraction peak positioned at Bragg angle  $2\theta$  (Fig. 4). In the case of  $\beta$ -CD and SA, PXRD patterns show a large number of peaks indicating crystallinity, but PXRD patterns of copolymer show no specific peaks. Crystalline intense signals of  $\beta$ -CD were observed at  $2\theta$  of  $4.7^\circ$ ,  $9.1^\circ$ ,  $10.7^\circ$ ,  $11.8^\circ$ ,  $14.9^\circ$ ,  $17.2^\circ$ ,  $19.8^\circ$  and  $23^\circ$ . In the case of SA, signals were observed at  $5.8^\circ$ ,  $10.2^\circ$ ,  $11.9^\circ$ ,  $14.1^\circ$ ,  $21.9$  and  $23.9^\circ$  which are consistent with previous records

(Flippen, 1973). However, the PXRD pattern of the copolymer confirmed the amorphous nature as expected for crosslinking and obtained behavior is in complete agreement with previously published reports on  $\beta$ -CD polymers (Li et al., 2016; Raoov et al., 2014).

#### 3.5. Specific surface area and porosity

To evaluate the internal microscopic structure of the copolymer, specific surface area (SSA) measurements and pore texture analysis were performed. Nitrogen adsorption/desorption technique was applied to determine the SSA and porous structure. The relevant textural parameter in term of SSA (obtained by applying BET method to the adsorption branch of the adsorption/desorption isotherm), mean pore diameter, and cumulative pore volume (obtained by analysis of the desorption branch using the BJH calculation method) are shown in Fig. 5. The BET surface area was recorded low as  $15.1\text{ m}^2\text{ g}^{-1}$  with a wide range of pore dimensions (5–100 nm). The obtained data suggested the mesoporous to microporous nature of this copolymer which is not very suitable to absorb nitrogen. These results are in consistent with previously reported literature for CD based crosslinked polymers. The pore size distribution of the  $\beta$ -CD-SA copolymer calculated from the adsorption branch of isotherms with the BJH approach indicated that copolymer exhibits a dominant pore diameter centered about 51 nm.

#### 3.6. Monomer composition ratio

Copolymers have been classified on the basis of chemical composition as well as molecular weight distribution. For SA chemical composition quantification, we herein developed HPLC method based on ELSD detector due to low baseline noise, accurate precision qualities of ELSD and suitability for detections of SA and CDs. Following ICH guideline for HPLC method validation, the method validated with linearity, specificity, and limit of detection (LOD), and limit of quantification (LOQ) parameters (Fig. S-1). From HPLC analysis, the composition of copolymer largely contributed by  $\beta$ -CD which holds the high compositional percentage over SA (Fig. 6). This differentiation

might be due to high reactivity of  $\beta$ -CD as compare to SA. The average content of SA was 5.52% (w/w) of the copolymer, which shows the average molar concentration in 100 molar copolymer solution contained 18 moles of SA and remaining 82 moles contain  $\beta$ -CD. Nevertheless, the detection amount is proved enough for the targeted effects in cellular experiments.

### 3.7. Drug adsorption

Dox was selected as a drug candidate to evaluate the cellular penetration ability of  $\beta$ -CD-SA copolymer. The supernatant layer method was adopted to investigate the adsorption/sequestration abilities of the copolymer towards Dox. The drug load-

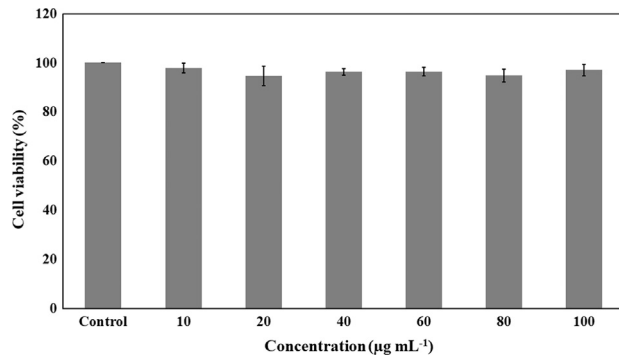


**Fig. 7** MTT assay data represent cytocompatible nature and no significant cytotoxic effect of the  $\beta$ -CD-SA copolymer on HeLa cells.

ing was checked by HPLC using the validated method used in our previous experiments (Singh et al., 2017). Drug loading capacity of the  $\beta$ -CD-SA copolymer namely, 1.13 % (w/w) recorded high as compared to only  $\beta$ -CD due to the contribution of external cavities formed by crosslinking of SA and  $\beta$ -CD (Fig. S-2). The drug loading capacity of copolymer demonstrates the amphiphilic nature of copolymer which can be used for the carrier of hydrophilic as well as hydrophobic drugs (characteristic properties of  $\beta$ -CD).

### 3.8. Cell viability study

MTT assay was performed to investigate the cytotoxicity of the  $\beta$ -CD-SA copolymer. The copolymer was exposed for 24 h, the samples were capable of metabolizing a dye (3-(4,5-dimethylthiazol-2yl)-2,5-diphenyl tetrazolium bromide) efficiently and the purple colored precipitate dissolved and analyzed spectrophotometrically. The viability of HeLa cells was tested at five different concentrations of the copolymer (Fig. 7). As a result, HeLa cells showed excellent viability at even high concentration. Cell viability assay indicated that the  $\beta$ -CD-SA copolymer did not have any toxic effect on HeLa cells over 24 h exposure and has good potentials for a pharmaceutical preparation.

### 3.9. In vitro cellular uptake study

To examine the cellular uptake efficiency, the Dox loaded copolymer was compared with free Dox under the same set

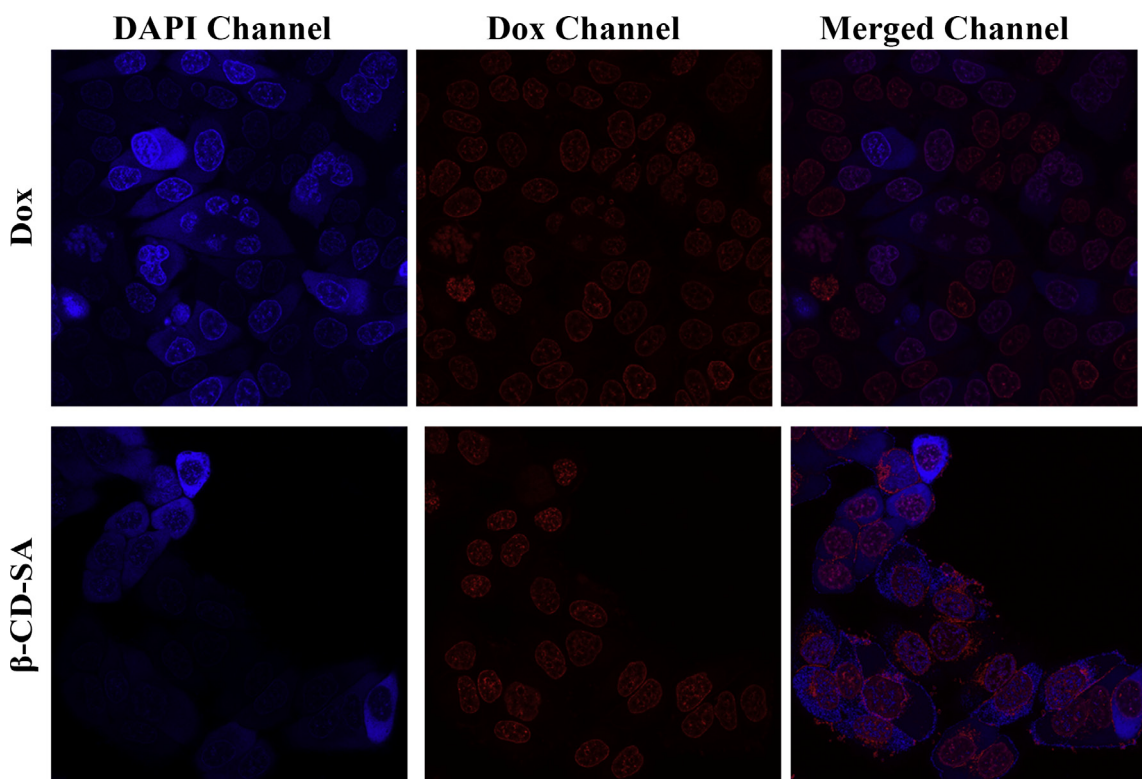


**Fig. 8** The confocal images of cellular uptake of  $\beta$ -CD-SA-copolymer particles and free Dox *in vitro*. The merged channel represents the fluorescence intensity of the Dox penetrated inside the cell nucleus which show the high amount of drug accumulate on the cell nucleus supporting the target properties of the copolymer.

of conditions. After 4 h of exposure, the copolymer particles can be easily located because of intracellular accumulation (Fig. 8) in DAPI labeled HeLa cells. The figures showed Dox-loaded  $\beta$ -CD-SA copolymer particles have good permeability and particles accumulated either at the wall or penetrate into the nucleus of cells. The Dox loaded  $\beta$ -CD-SA copolymer showed strong Dox fluorescence in nuclei after 4 h exposure, indicating internalization of Dox. The Dox fluorescence intensity and accumulation of particles on the cell nuclei are more evidence for targeting and enhancing cellular uptake. Possibly, SA played a role in promoting cell internalization of Dox as reported previously (Bader and Wardwell, 2014).

#### 4. Conclusions

The synthesis of the  $\beta$ -CD-SA copolymer was inspired by the high drug encapsulation and inclusion efficiency of  $\beta$ -CD for drug molecules and site specific targeting properties of SA. The copolymer of  $\beta$ -CD and SA was successfully synthesized by crosslinking approach aimed at targeting function and high cellular penetration. The copolymer possesses the amorphous nature and better thermal stability when compared with  $\beta$ -CD or SA. Cell viability assay demonstrates that  $\beta$ -CD-SA copolymer does not have a significant cytotoxic effect on HeLa cells. What's more, the obtained copolymer has good drug loading capacity for Dox and high cellular penetration ability as compare to  $\beta$ -CD. In summary, integrated with both of, the loading capacity of CDs and the targeting function of SA, the resultant copolymer can be a novel effective carrier for targeted drug delivery.

#### Acknowledgements

The authors are grateful for the financial support from the National Natural Science Foundation of China (No. 81430087) and National Science and Technology Major Project (2017ZX09101001-006). We gratefully acknowledged the staff from BL01B beamline of National Facility for Protein Science Shanghai (NFPS) at Shanghai Synchrotron Radiation Facility, for assistance during data collection.

#### Appendix A. Supplementary material

Supplementary data associated with this article can be found, in the online version, at <https://doi.org/10.1016/j.arabjc.2017.11.011>.

#### References

Alupei, V., Alupei, I.C., Ritter, H., 2005. Cyclodextrins in polymer modification: Diels-Alder addition of cyclopentadiene/methylated- $\beta$ -cyclodextrin complex on unsaturated polyester and formation of a new type of polypseudorotaxane. *Macromol. Rapid Commun.* 26, 40–45.

Ansari, K.A., Torne, S.J., Vavia, P.R., Trotta, F., Cavalli, R., 2011. Paclitaxel loaded nanosponges: in-vitro characterization and cytotoxicity study on MCF-7 cell line culture. *Curr. Drug Deliv.* 8, 194–202.

Bader, R.A., Wardwell, P.R., 2014. Polysialic acid: overcoming the hurdles of drug delivery. *Therapeutic Deliv.* 5, 235–237.

Binello, A., Robaldo, B., Barge, A., Cavalli, R., Cravotto, G., 2008. Synthesis of cyclodextrin-based polymers and their use as debittering agents. *J. Appl. Polym. Sci.* 107, 2549–2557.

Bondioli, L., Costantino, L., Ballestrazzi, A., Lucchesi, D., Boraschi, D., Pellati, F., Benvenuti, S., Tosi, G., Vandelli, M.A., 2010. PLGA nanoparticles surface decorated with the sialic acid, N-acetylneurameric acid. *Biomaterials* 31, 3395–3403.

Bull, C., Heise, T., van Hilt, N., Pijnenborg, J.F., Bloemendaal, V., Gerrits, L., Kers-Rebel, E.D., Ritschel, T., den Brok, M.H., Adema, G.J., Boltje, T.J., 2017. Steering Siglec-Sialic Acid Interactions on Living Cells using Bioorthogonal Chemistry. *Angewandte Chemie (International ed. in English)*.

Buttner, B., Kannicht, C., Schmidt, C., Loster, K., Reutter, W., Lee, H.Y., Nohring, S., Horstkorte, R., 2002. Biochemical engineering of cell surface sialic acids stimulates axonal growth. *J. Neurosci.* 22, 8869–8875.

Cavalli, R., Akhter, A.K., Bisazza, A., Giustetto, P., Trotta, F., Vavia, P., 2010. Nanosponge formulations as oxygen delivery systems. *Int. J. Pharmaceut.* 402, 254–257.

Chen, P., Liang, H.W., Lv, X.H., Zhu, H.Z., Yao, H.B., Yu, S.H., 2011. Carbonaceous nanofiber membrane functionalized by beta-cyclodextrins for molecular filtration. *ACS Nano* 5, 5928–5935.

Crini, G., 2014. Review: a history of cyclodextrins. *Chem. Rev.* 114, 10940–10975.

Darandale, S.S., Vavia, P.R., 2013. Cyclodextrin-based nanosponges of curcumin: formulation and physicochemical characterization. *J. Incl. Phenom. Macrocycl. Chem.* 75, 315–322.

Eastman, 1998. Vitamin E TPGS, Properties and Applications. Eastman, USA Publication EFC-226A.

Flippen, J., 1973. The crystal structure of [beta]-d-N-acetylneurameric acid dihydrate (sialic acid), C11H19NO9.2H2O. *Acta Crystallogr. Sect. B* 29, 1881–1886.

Freeman, R., Boekhoven, J., Dickerson, M.B., Naik, R.R., Stupp, S.I., 2015. Biopolymers and supramolecular polymers as biomaterials for biomedical applications. *Mrs Bull.* 40, 1089–1101.

Gil, E.S., Wu, L.F., Xu, L.C., Lowe, T.L., 2012.  $\beta$ -Cyclodextrin-poly(beta-amino ester) nanoparticles for sustained drug delivery across the blood-brain barrier. *Biomacromolecules* 13, 3533–3541.

Hare, J.I., Lammers, T., Ashford, M.B., Puri, S., Storm, G., Barry, S. T., 2017. Challenges and strategies in anti-cancer nanomedicine development: an industry perspective. *Adv Drug Deliv. Rev.* 108, 25–38.

Hirayama, F., Uekama, K., 1999. Cyclodextrin-based controlled drug release system. *Adv. Drug Deliv. Rev.* 36, 125–141.

Hirotsu, T., Higashi, T., Motoyama, K., Arima, H., 2017. Cyclodextrin-based sustained and controllable release system of insulin utilizing the combination system of self-assembly PEGylation and polypseudorotaxane formation. *Carbohydr. Polym.* 164, 42–48.

Kettel, M.J., Hildebrandt, H., Schaefer, K., Moeller, M., Groll, J., 2012. Tenside-free preparation of nanogels with high functional  $\beta$ -cyclodextrin content. *ACS Nano* 6, 8087–8093.

Lee, J.H., Jun, Y.W., Yeon, S.I., Shin, J.S., Cheon, J., 2006. Dual-mode nanoparticle probes for high-performance magnetic resonance and fluorescence imaging of neuroblastoma. *Angew. Chem.* 45, 8160–8162.

Li, H., Meng, B., Chai, S.-H., Liu, H., Dai, S., 2016. Hyper-crosslinked [small beta]-cyclodextrin porous polymer: an adsorption-facilitated molecular catalyst support for transformation of water-soluble aromatic molecules. *Chem. Sci.* 7, 905–909.

Lo Meo, P., Lazzara, G., Liotta, L., Riela, S., Noto, R., 2014. Cyclodextrin-calixarene co-polymers as a new class of nanosponges. *Polym. Chem.-UK* 5, 4499–4510.

Mendez-Ardoy, A., Guilloteau, N., Di Giorgio, C., Vierling, P., Santoyo-Gonzalez, F., Mallet, C.O., Fernandez, J.M.G., 2011.  $\beta$ -Cyclodextrin-based polycationic amphiphilic “Click” clusters: effect of structural modifications in their DNA complexing and delivery properties. *J. Org. Chem.* 76, 5882–5894.

Minelli, R., Cavalli, R., Ellis, L., Pettazzoni, P., Trotta, F., Ciamporcero, E., Barrera, G., Fantozzi, R., Dianzani, C., Pili, R., 2012. Nanospunge-encapsulated camptothecin exerts anti-tumor activity in human prostate cancer cells. *Eur. J. Pharm. Sci.* 47, 686–694.

Minotti, G., Menna, P., Salvatorelli, E., Cairo, G., Gianni, L., 2004. Anthracyclines: molecular advances and pharmacologic developments in antitumor activity and cardiotoxicity. *Pharmacol. Rev.* 56, 185–229.

O'Mahony, A.M., Godinho, B.M.D.C., Ogier, J., Devocelle, M., Darcy, R., Cryan, J.F., O'Driscoll, C.M., 2012. Click-modified cyclodextrins as nonviral vectors for neuronal siRNA delivery. *Ac. Chem. Neurosci.* 3, 744–752.

Oba, K., Ishida, Y., Ito, Y., Ohtani, H., Tsuge, S., 2000. Characterization of branching and/or cross-linking structures in polycarbonate by reactive pyrolysis–gas chromatography in the presence of organic alkali. *Macromolecules* 33, 8173–8183.

Perillo, N.L., Marcus, M.E., Baum, L.G., 1998. Galectins: versatile modulators of cell adhesion, cell proliferation, and cell death. *J. Mol. Med.* 76, 402–412.

Ping, Y., Liu, C.D., Zhang, Z.X., Liu, K.L., Chen, J.H., Li, J., 2011. Chitosan-graft-(PEI-beta-cyclodextrin) copolymers and their supramolecular PEGylation for DNA and siRNA delivery. *Biomaterials* 32, 8328–8341.

Rao, M., Bajaj, A., Khole, I., Munjapara, G., Trotta, F., 2013. In vitro and in vivo evaluation of beta-cyclodextrin-based nanospanges of telmisartan. *J. Incl. Phenom. Macrocycl. Chem.* 77, 135–145.

Raoov, M., Mohamad, S., Abas, M.R., 2014. Synthesis and Characterization of  $\beta$ -cyclodextrin functionalized ionic liquid polymer as a macroporous material for the removal of phenols and As(V). *Int. J. Mol. Sci.* 15, 100–119.

Rudra, J.S., Tripathi, P.K., Hildeman, D.A., Jung, J.P., Collier, J.H., 2010. Immune responses to coiled coil supramolecular biomaterials. *Biomaterials* 31, 8475–8483.

Russo, M., Saladino, M.L., Martino, D.C., Lo Meo, P., Noto, R., 2016. Polyaminocyclodextrin nanospanges: synthesis, characterization and pH-responsive sequestration abilities. *Rsc Adv.* 6, 49941–49953.

Shi, J.J., Kantoff, P.W., Wooster, R., Farokhzad, O.C., 2017. Cancer nanomedicine: progress, challenges and opportunities. *Nat. Rev. Cancer* 17, 20–37.

Singh, V., Guo, T., Wu, L., Xu, J., Liu, B., Gref, R., Zhang, J., 2017. Template-directed synthesis of a cubic cyclodextrin polymer with aligned channels and enhanced drug payload. *Rsc Adv.* 7, 20789–20794.

Sultana, R., Di Domenico, F., Tseng, M., Cai, J.A., Noel, T., Chelvarajan, R.L., Pierce, W.D., Cini, C., Bondada, S., St Clair, D. K., Butterfield, D.A., 2010. Doxorubicin-induced thymus senescence. *J. Proteome Res.* 9, 6232–6241.

Torne, S., Darandale, S., Vavia, P., Trotta, F., Cavalli, R., 2013. Cyclodextrin-based nanospanges: effective nanocarrier for Tamoxifen delivery. *Pharm. Dev. Technol.* 18, 619–625.

Trotta, F., Zanetti, M., Cavalli, R., 2012. Cyclodextrin-based nanospanges as drug carriers. *Beilstein J. Org. Chem.* 8, 2091–2099.

Uekama, K., 1999. Cyclodextrins in drug delivery system – preface. *Adv. Drug Deliv. Rev.* 36, 1–2.

Wang, H., Liu, K., Chen, K.J., Lu, Y.J., Wang, S.T., Lin, W.Y., Guo, F., Kamei, K.I., Chen, Y.C., Ohashi, M., Wang, M.W., Garcia, M. A., Zhao, X.Z., Shen, C.K.F., Tseng, H.R., 2010. A rapid pathway toward a superb gene delivery system: programming structural and functional diversity into a supramolecular nanoparticle library. *Ac. Nano* 4, 6235–6243.

Webber, M.J., Appel, E.A., Meijer, E.W., Langer, R., 2016. Supramolecular biomaterials. *Nat. Mater.* 15, 13–26.

Xu, Z.G., Liu, S.Y., Liu, H., Yang, C.J., Kang, Y.J., Wang, M.F., 2015. Unimolecular micelles of amphiphilic cyclodextrin-core star-like block copolymers for anticancer drug delivery. *Chem. Commun.* 51, 15768–15771.

Zhang, D., Pan, X.L., Wang, S., Zhai, Y.L., Guan, J.B., Fu, Q., Hao, X.L., Qi, W.P., Wang, Y.L., Lian, H., Liu, X.H., Wang, Y.J., Sun, Y.H., He, Z.G., Sun, J., 2015. Multifunctional poly(methyl vinyl ether-co-maleic anhydride)-graft-hydroxypropyl-beta-cyclodextrin amphiphilic copolymer as an oral high-performance delivery carrier of tacrolimus. *Mol. Pharmaceut.* 12, 2337–2351.